Characterization of piezoelectric device for implanted pacemaker energy harvesting

Sunny Jay, Manuel Caballero, William Quinn, John Barrett, Martin Hill

Cork Institute of Technology, Bishopstown, Cork, Ireland.

sunny.jay@mycit.ie

Abstract. Novel implanted cardiac pacemakers that are powered by energy harvesters driven by the cardiac motion and have a 40 year lifetime are currently under development. To satisfy space constraints and energy requirements of the device, silicon-based MEMS energy harvesters are being developed in the EU project (MANpower[1]). Such MEMS harvesters for vibration frequencies below 50 Hz have not been widely reported. In this paper, an analytical model and a 3D finite element model (FEM) to predict displacement and open circuit voltage, validated through experimental analysis using an off-the-shelf low frequency energy harvester, are presented. The harvester was excited through constant amplitude sinusoidal base displacement over a range of 20 to 70 Hz passing through its first mode natural frequency at 47 Hz. At resonance both models predict displacements with an error of less than 2% when compared to the experimental result. Comparing the two models, the application of the experimentally measured damping ratio differs for accurate displacement prediction and the differences in symmetry in the measured and modelled displacement and voltage data around the resonance frequency indicate the two piezoelectric voltage models use different fundamental equations.

1. Introduction

The human heart has a natural pacemaker called the sino-atrial (SA) node, which sends an electrical pulse through nerves around the muscle tissue causing them to contract [1]. However, if this begins to fail an artificial pacemaker is required to provide pacing. Conventional pacemakers require battery power to last the 5 to 10 year life expectancy of the device [2]. With the power densities available, these batteries are too large to suit an implanted intracardiac pacemaker. This necessitates pacing leads as shown in Figure 1-1 [3], these often cause discomfort and infection for the patient, along with electrical issues such as insulation deterioration and lead fractures [4]. This problem could be overcome if it were possible to harvest the mechanical energies from the heartbeat using an embedded energy harvester. Embedded energy harvesting has provoked more and more interest in recent years as the desire to have portable, wireless or embedded technology increases. Piezoelectric materials have received much attention due to their ability to convert mechanical strain directly into electrical energy. However, much of this work has focused on higher frequency ranges above 100 Hz as it is difficult to generate usable energy from lower frequency vibration sources as energy is an accumulation of power over a number of cycles and a low cycle rate means a low accumulation rate. Since the main energy in the vibration spectrum of the beating human heart is concentrated below 50 Hz, there has been little development of energy harvesters targeted at this application.

[1] The authors would like to thank the MANpower consortium for their contribution. The research leading to these results was funded from the European Union Seventh Framework Program (FP7-NMP-2013-SMALL-7) under the grant agreement No. 604360.

In addition to the low vibration frequencies, the confined space in the human heart, the shape of the ventricles and the requirement to implant the intracardiac pacemaker through a vein constrain the pacemaker shape to a cylinder less than 6mm diameter and 40mm in length. This cylinder has to also contain all the conventional pacing electronics, leaving only very limited space for an embedded energy harvester that needs to generate power in the 5-10μW range [5], [6]. The circular cross-section of the cylinder also limits the maximum displacement of a planar MEMS harvester. These combined constraints have demanded a novel harvester and new approaches to design, modelling, fabrication and testing [7].

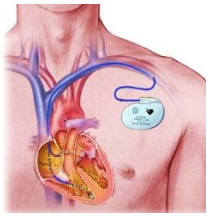

Figure 1-1 Conventional pacemaker location

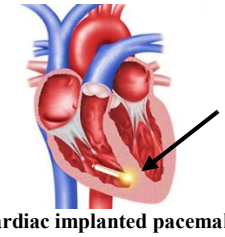

Figure 1-2 Intracardiac implanted pacemaker location [8]

To predict the power capabilities and reliability of such a device and to explore the full design space, accurate models are essential. This paper reports the successful development of two models, validated by experiment, capable of accurately predicting the displacement and open circuit voltage of a commercial off the shelf (COTS) clamped-free cantilever type piezoelectric energy harvester similar in size and operating frequency to the intracardiac harvester. These verified models can now be used to fully explore the design space of the required harvester.

2. Experimental Set Up

A thin film piezoelectric energy harvester was purchased for characterization. The device has a polyvinylidene fluoride (PVDF) core laminated in a sheet of polyester (Mylar) and is a simple cantilever beam type harvester.

Figure 2-1 Thin Film Energy Harvester

The device was subject to a harmonic vertical base excitation provided by an electromagnetic shaker (LDS V450 - Permanent Magnet Shaker). Apart from the physical dimensions of the harvester, the resonant frequency, damping, capacitance and impedance were measured before any response to base excitations was studied. The total thickness was measured using a digital micrometre, (MITUTOYO Series 293-344 Digimatic Micrometer (IP-65)). The damped resonant frequency was measured by clamping the base to a rigid support and subjecting the free end to an impulse. A laser displacement sensor (Micro Epsilon optoNCDT 1420 - Smart Laser Triangulation Displacement Sensor) was used in combination with a high speed camera (FASTCAM SA1.1 photron) to record the oscillations. From this the damped resonant frequency and damping ratio could be extracted. The capacitance and impedance of the energy harvester were measured using an impedance analyser (HP 4192A LF). With these values the thickness of the PVDF could be calculated using equation (2.1)

$$C = \frac{\mathcal{E}_0 \mathcal{E}_r A}{t_p} \quad \gg \quad t_p = \frac{\mathcal{E}_0 \mathcal{E}_r A}{C} \tag{2.1}$$

Where $\mathcal{E}_0$ is the permittivity of free space, $\mathcal{E}_r$ is the relative permittivity, C is the capacitance, A is the area of piezoelectric material and t_p is the PVDF thickness. As the harvester had two metal rivets at the base to attach the lead wires, a rubber sheath was fashioned in order to clamp it to the shaker without causing a short circuit across the terminals. The harvester was subjected to a base excitation of 1 mm peak to peak at frequencies sweeping through its first resonant mode. At incremental frequency steps

the tip displacement and open circuit AC voltage produced were recorded, using laser displacement sensors and an oscilloscope (Aglient Technologies DS01022A).

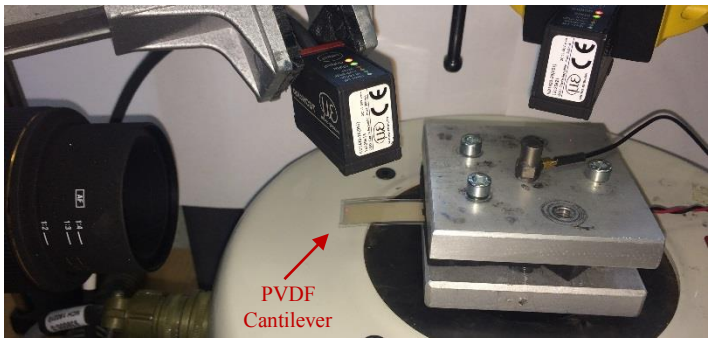

Figure 2-2 Experimental Set Up

3. Modelling PVDF Unimorph Sensor

Unimorph piezoelectric cantilever beams can be modelled using composite beam equations. Based on the mechanics of vibrating beams, piezoelectric energy conversions and fundamental circuit theory accurate models were previously reported [9]. The three most commonly used analytical models are Pin-Force, Enhanced Pin-Force and Euler-Bernoulli [10]. The Euler-Bernoulli method is reported as the most accurate of the three methods and for this reason is used for this work [11]. The PVDF and substrate are modelled to have a perfect bond and both bend about a common neutral axis. This neutral axis is calculated using a weighted Young's modulus approach. The strain is modelled to increase linearly, with thickness, through the composite beam [11]–[13].

Cantilever Beam Modelling

Table 3-1 Unimorph Cantilever beam Parameters

	Parameter	***Energy Harvester***
Beam	***Length (m) L***	*0.032*
	Width (m) b	*0.01219*
	Thickness (m) t_b	*0.000194*
	Material	*Polyester (Mylar)*
	Density (kg/m^3)	*1390*
	Young's Modulus (GPa) E_b	*4.9*
PVDF	***Length (m) l_p***	*0.03*
	Width (m) b	*0.01219*
	Thickness (m) t_p	*0.000045*
	Material	*PVDF*
	Density (kg/m^3)	*1780*
	Young's Modulus (GPa) E_p	*1.1*
	Voltage Constant g31 (Vm/N)	*0.281*

In order to use the voltage estimation model the harvester was first modelled as composite cantilever beam. A free clamped beam was modelled with a harmonic base excitation and tip mass. Although the harvester did not have a tip mass, this was satisfied by setting the mass value to 0. The properties of the harvester are listed in Table 3-1 and the cantilever beam model is shown in Figure 3-1. The governing equation of a clamped-free cantilever beam with a tip mass excited through base excitation with structural and air damping is

$$E_b I_b \frac{\partial^4 \mathrm{w}_{rel}(x,t)}{\partial t^4} + c_s I_b \frac{\partial^5 \mathrm{w}_{rel}(x,t)}{\partial x^4} + c_a \frac{\partial \mathrm{w}_{rel}(x,t)}{\partial \mathrm{t}} + m \frac{\partial^2 \mathrm{w}_{rel}(x,t)}{\partial t^2} = -[m + M_t \delta(x - L_b)] \frac{\partial^2 \mathrm{w}_b(x,t)}{\partial t^2} \tag{3.1}$$

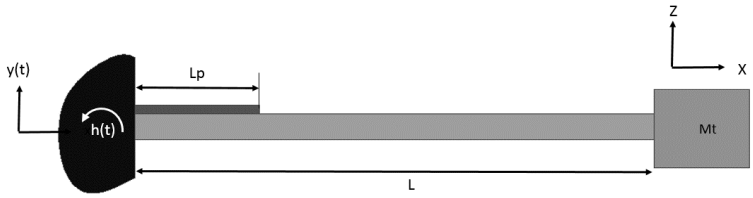

Figure 3-1 Cantilever Beam Model

Where $w_{rel}(x,t)$ is the relative displacement between the cantilever tip and the base, $w_b(x,t)$ is the displacement of the base, m is the mass per unit length and M_t is the tip mass. c_s is the Kelvin-Voigt or strain rate damping and c_a is the viscous air damping.The absolute displacement of the beam can be expressed as

$$w(x,t) = w_{rel}(x,t) + w_b(x,t) \tag{3.2}$$

The base displacement $w_b(x,t)$ is input as a sinusoidal function and the relative displacement with respect to time and position can be calculated using the modal shape and the modal coordinate equation.

$$w_{rel}(x,t) = \sum_{i=1}^{n} q_i(t)\, Z_i(x) \tag{3.3}$$

The *ith* modal shape is denoted as $Z_i(x)$ while the *ith* modal coordinate equation is $q_i(t)$. For a cantilever beam with a tip mass the modal shape can be calculated using the beam parameters and material properties [10], [11], [14]. The amplitude of the modal coordinate equation is heavily dependent on damping ratio ζ which was measured experimentally.

$$q_i(t) = \frac{1}{\omega_d} \int_0^t F_i(\tau) e^{-\zeta\omega(t-\tau)} \sin\big(\omega_d(t-\tau)\big)\, d\tau \tag{3.4}$$

Since the base can be assumed to have very little rotation *(h(t) = 0)* [14]–[16], and only be excited by vertical vibrations the force equation can be simplified to

$$F(t) = -m\left(\frac{d^2y(t)}{dt^2}\int_0^L Z_i(x)dx\right) - M_t Z_i(L)\left(\frac{d^2y(t)}{dt^2}\right) \tag{3.5}$$

The relative displacement was then calculated using equation (3.3). The curvature of the beam was found by differentiating the displacement twice with respect to time. The average curvature was then evaluated as

$$k_{ave}(t) = \frac{1}{L_p}\int_0^{L_p} k(x,t)dx \tag{3.6}$$

Finally the average moment acting on the PVDF was calculated using

$$M(t) = E_b I_b k_{ave}(t) \tag{3.7}$$

Maximum Voltage Estimation

The maximum voltage will occur under open circuit conditions, this value was predicted using the Euler-Bernoulli voltage equation

$$Veb = -\frac{6g_{31}\left(\frac{E_b t_b}{E_p t_p}\right)\left(1+\frac{t_b}{t_p}\right)M}{bt_p\left[1+\left(\frac{E_b t_b}{E_p t_p}\right)^2\left(\frac{t_b}{t_p}\right)^2 + 2\frac{E_b t_b}{E_p t_p}\left(2+3\frac{t_b}{t_p}+2\left(\frac{t_b}{t_p}\right)^2\right)\right]} \tag{3.8}$$

Computer Simulation

The harvester was also modelled using the FEM software COMSOL Mutiphysics. The computer simulations gave a very clear visual representation of the cantilever beam response and gave a comparison between 2 dimensional and 3 dimensional modelling. The two models were developed with

the same parameters and subjected to the same base excitation. The model was run in the frequency domain with a fixed support at the base and all other domains free.

4. Results

The damping was calculated both by fitting an exponential decay curve to the recorded displacement data, and using equation (4.1):

$$\frac{n_{th}+1}{n_{th}} = \exp\left[\frac{-2\zeta\pi}{\sqrt{1-\zeta^2}}\right] \tag{4.1}$$

Where n_{th} and $n_{th}+1$ are the amplitude of successive oscillations of the beam once the initial chaotic response from the impulse has settled and ζ is the damping ratio. Both methods gave the same damping ratio of 0.05.

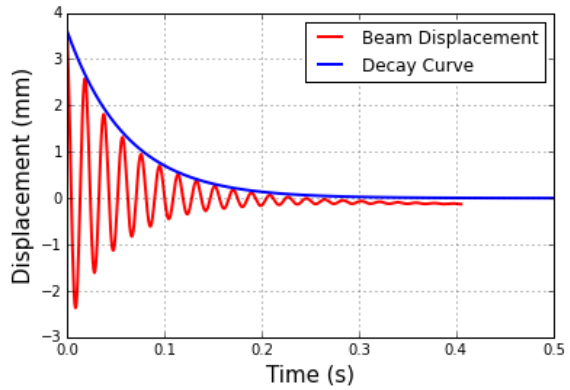

Figure 4-1 Response to impulse, Damping ratio = 0.05

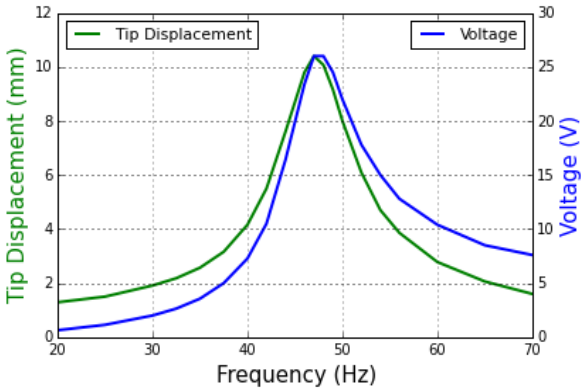

Figure 4-2 Response to 1 mm base excitation frequency sweep.

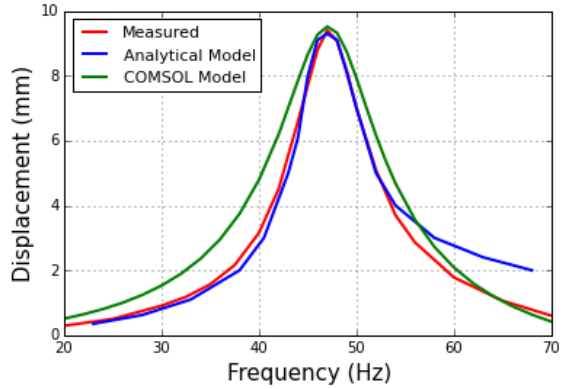

Figure 4-3 Measured and modelled displacements

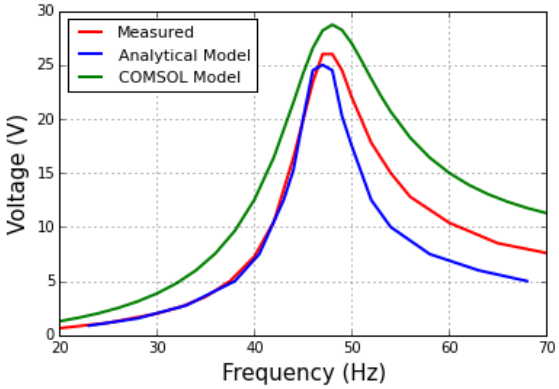

Figure 4-4 Measured and modelled Voltages

Figure 4-2 shows the raw recorded data of the energy harvesters' response to a 1 mm peak to peak base excitation frequency sweep. All results are peak to peak values. The measured displacements are total displacement, this was corrected to the relative tip displacement by subtracting the base displacement from the total tip displacement taking into account the phase shift. In order to match displacement amplitude, the COMSOL model required a damping ratio of 0.1, higher than the measured value.

5. Discussion

Figure 4-3 shows that both the analytical and COMSOL models are very accurate at predicting tip displacement at resonance. The COMSOL models accuracy decreases either side of the resonant frequency while the analytical model remains very accurate up to 53 Hz. A damping ratio cannot be input directly into COMSOL, Rayleigh damping coefficients had to be calculated in order to damp the

model. The COMSOL model required higher damping than the measured values to match the displacement amplitudes and there is ongoing work trying to solve this issue. The measured data shows an increase in voltage for a given displacement at higher frequencies compared to lower frequencies. The COMSOL model also predicts this, but exceeds the recorded voltage. Conversely, the analytical model predicts voltages directly from displacements levels, indicating the two models work off different fundamental equations. The analytical model predicts the voltage accurately until resonance. After this it consistently predicts a lower voltage than the recorded value. This may be because the analytical model predicts that the beam will resonate only at its first mode shape, and in reality as it reaches higher frequencies there may be some torsional rotations causing higher strain levels on the device and in turn creating higher voltages. It was noted that overall both models are most accurate at resonance which suits the required application. For an implanted pacemaker the main source of available energy is an impulse from the heartbeat. This would result in a response similar to Figure 4-1.The device will most likely vibrate at its resonant frequency with a decaying amplitude. Future work will look at heartbeat acceleration profiles, and use modelling to predict how much power can be generated from each impulse.

6. Conclusion

In this paper analytical and 3D FEM electromechanical models of a microscale energy harvester were presented. The application for the modelled device is to operate on the low frequency range produced by cardiac motion on which little previous work was reported. The models make accurate displacement and voltage predictions at resonance compared to experimental COTS device measurements. However, for vibration inputs at non resonant frequencies both modelling approaches yield different output voltages suggesting they use different fundamental equations. In addition, the FEM model requires a damping ratio twice as large as the measured value in order to achieve the same displacement amplitude while the analytical model can have the measured value input unmodified. Both models will be developed further to predict the power capabilities of a MEMS energy harvester in an implanted cardiac pacemaker.

7. References

[1] R. W. Joyner and F. J. van Capelle, “Propagation through electrically coupled cells. How a small SA node drives a large atrium.,” *Biophys. J.*, vol. 50, no. 6, pp. 1157–1164, Dec. 1986.
[2] V. S. Mallela, V. Ilankumaran, and N. S. Rao, “Trends in Cardiac Pacemaker Batteries,” *Indian Pacing Electrophysiol. J.*, vol. 4, no. 4, pp. 201–212, Oct. 2004.
[3] V. L. Paone S, Trimaglio F, Migliore A, Maltoni S, “Transcatheter implantable miniaturised leadless pacemakers [Internet].,” Agenas, Agnezia nazionale per i servizi sanitari regionali, No. 17, Dec. 2014.
[4] R. E. Kirkfeldt, J. B. Johansen, E. A. Nohr, M. Moller, P. Arnsbo, and J. C. Nielsen, “Risk factors for lead complications in cardiac pacing: A population-based cohort study of 28,860 Danish patients,” *Heart Rhythm*, vol. 8, no. 10, pp. 1622–1628, Oct. 2011.
[5] M. Deterre, *Toward an energy harvester for leadless pacemakers*. Paris 11, 2013.
[6] M. Deterre, B. Boutaud, R. Dalmolin, S. Boisseau, J. J. Chaillout, E. Lefeuvre, and E. Dufour-Gergam, “Energy harvesting system for cardiac implant applications,” in *2011 Symposium on Design, Test, Integration and Packaging of MEMS/MOEMS (DTIP)*, 2011, pp. 387–391.
[7] N. Jackson, R. O’Keeffe, F. Waldron, M. O’Neill, and A. Mathewson, “Evaluation of low-acceleration MEMS piezoelectric energy harvesting devices,” *Microsyst. Technol.*, vol. 20, no. 4–5, pp. 671–680, Dec. 2013.
[8] V. Y. Reddy, R. E. Knops, J. Sperzel, M. A. Miller, J. Petru, J. Simon, L. Sediva, J. R. de Groot, F. V. Y. Tjong, P. Jacobson, A. Ostrosff, S. R. Dukkipati, J. S. Koruth, A. A. M. Wilde, J. Kautzner, and P. Neuzil, “Permanent Leadless Cardiac Pacing Results of the LEADLESS Trial,” *Circulation*, vol. 129, no. 14, pp. 1466–1471, Apr. 2014.
[9] D. J. I. A. Erturk, “A Distributed Parameter Electromechanical Model for Cantilevered Piezoelectric Energy Harvesters,” *J. Vib. Acoust.*, vol. 130, no. 4, 2008.
[10] R. R. Muppala, K. P. Raju, N.-M. Moon, and B.-H. Jung, “Analytical Models to Predict Power Harvesting with Piezoelectric Transducer,” *J. Korean Inst. Electromagn. Eng. Sci.*, vol. 8, no. 1, pp. 6–11, Mar. 2008.
[11] T. Eggborn, “Analytical Models to Predict Power Harvesting with Piezoelectric Materials,” thesis, Virginia Tech, 2003.
[12] K. L. Bing, T. Li, H. H. Hng, F. Boey, T. Zhang, and S. Li, *Waste Energy Harvesting: Mechanical and Thermal Energies*. Springer Science & Business Media, 2014.
[13] N. Jalili, *Piezoelectric-Based Vibration Control: From Macro to Micro/Nano Scale Systems*. Springer Science & Business Media, 2009.
[14] A. Erturk and D. J. Inman, *Piezoelectric Energy Harvesting*, 1 edition. Chichester: Wiley, 2011.
[15] A. Erturk and D. J. Inman, “An experimentally validated bimorph cantilever model for piezoelectric energy harvesting from base excitations,” *Smart Mater. Struct.*, vol. 18, no. 2, p. 25009, 2009.
[16] F. Häggström, J. Gustafsson, and J. Delsing, “Piezoelectric energy harvesting modeled with SPICE,” *Submitt. IEEE Sens. J. Vol*.